

# Causal Discovery-Driven Change Point Detection in Time Series

Shanyun Gao<sup>1</sup>, Raghavendra Addanki<sup>2</sup>, Tong Yu<sup>2</sup>, Ryan A. Rossi<sup>2</sup>, Murat Kocaoglu<sup>1</sup>

<sup>1</sup> Purdue University, West Lafayette, USA

<sup>2</sup> Adobe Research, San Jose, USA



## Motivations

Traditionally, change detection focuses on shifts in **the joint distribution** of all variables—capturing system-wide changes but missing **local changes** in specific variables. Such localized changes often carry more real-world significance.

Moreover, many existing methods rely on the assumption of independently and identically distributed (IID) samples, which may not hold in practice.

## Our Goal

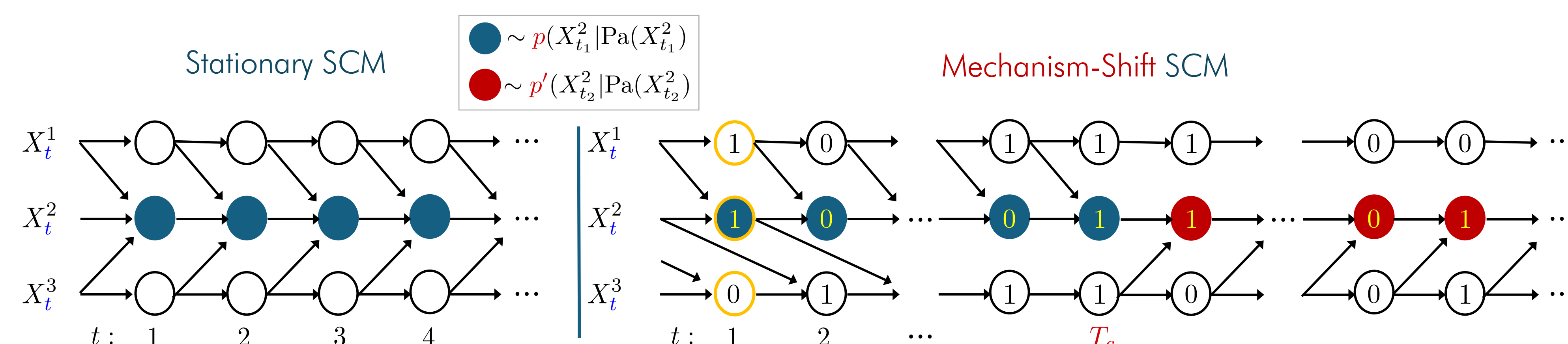
*Can we detect changes targeting the underlying **causal mechanisms** of a time series—rather than joint or marginal distributional shifts—with theoretical guarantees and without assuming IID samples?*

## Key Idea

Phase One (causal discovery) focuses on uncovering the underlying causal structure of the entire non-stationary time series.

Phase Two (change point detection) centers on change point detection within each time series segment, using the causal structures estimated in Phase One to guide the segmentation.

## Union of Parent Sets in Non-Stationary Time Series



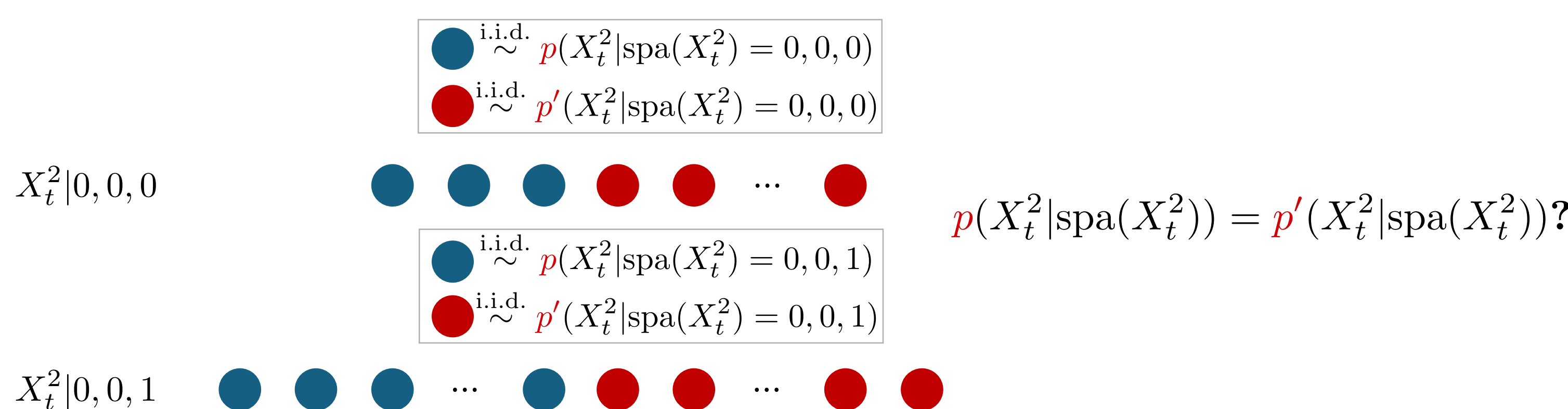
Theorem (adapted from [1]). *Let  $\text{SPA}(X_t^j)$  denote the union parent set of  $X_t^j$  and  $\widehat{\text{SPA}}(X_t^j)$  denote the estimated union parent set obtained from PCMCi [2] algorithm on time series  $\mathbf{X}^j$  with a Mechanism-Shift SCM. Under certain assumptions and with an oracle (infinite sample size limit), we have that:*

$$\text{SPA}(X_t^j) \subseteq \widehat{\text{SPA}}(X_t^j)$$

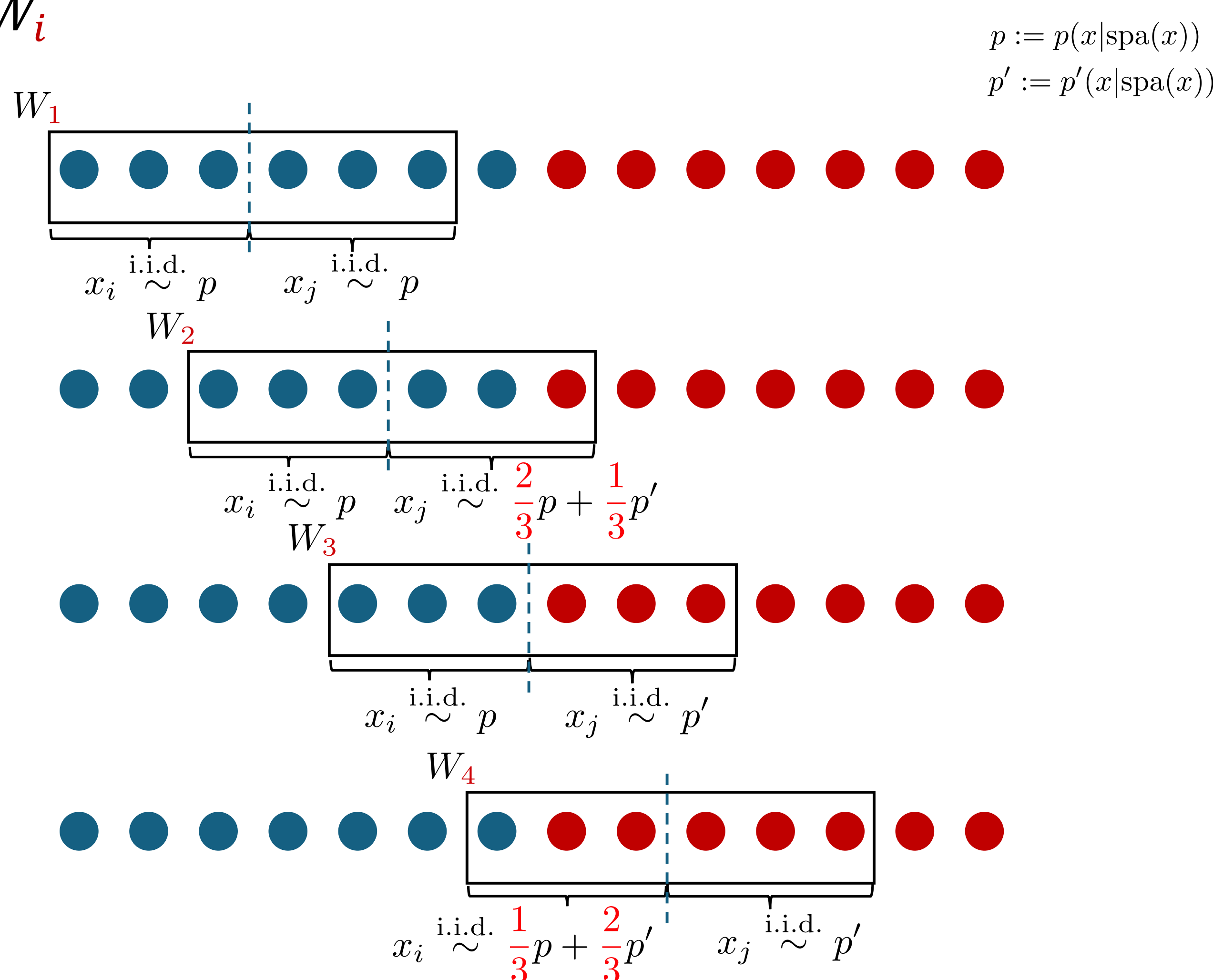
## Causal-RuLSIF: Change Point Detection

Definition [Time Series Segments]. *A collection of non-overlapping, non-empty subsets of a univariate, discrete-valued time series  $\mathbf{X}^j \in V$  governed by a Mechanism-Shift SCM, where all segments share the same union parent set  $\text{SPA}(X_t^j)$  over a fixed domain, but differ in their configurations  $\text{spa}(X_t^j)$ .*

Samples in each Time Series Segment of  $\mathbf{X}^2$  are IID.



## Dynamic $\alpha$ -Relative Pearson Divergence $PE_{\alpha_i}$ via Sliding Window $W_i$



One of the two sample sets from each half of the sliding window follows a mixture distribution of the form  $(1 - \alpha_i)p + \alpha_i p'$ , assuming one change point per window.

$\alpha_i$   $\propto$  the concentration of  $p'$  in such mixture distribution which depends on the window index  $i$ .

Instead of a fixed hyperparameter  $\alpha$ , we have a dynamic parameter  $\alpha_i$  that corresponds to the sliding window  $W_i$ .

Dynamic  $\alpha$ -relative density-ratio:

$$r_{\alpha_i}(x | \text{spa}(x)) = \frac{p}{(1 - \alpha_i)p + \alpha_i p'} := \frac{p}{q_{\alpha_i}}$$

Dynamic  $\alpha$ -relative Pearson Divergence and its Estimator:

$$PE_{\alpha_i}[p, p'] := \frac{1}{2} \mathbb{E}_{x \sim q_{\alpha_i}} [(r_{\alpha_i}(x | \text{spa}(x)) - 1)^2]$$

where  $PE_{\alpha_i}$  is estimated from a method called RuLSIF [3,4] with kernel functions.

Theorem. *Let  $\{\widehat{PE}_{\alpha_i}\}_i$  be the estimated PE series for one time series segment  $X^j(\Lambda) \subsetneq \mathbf{X}^j \subsetneq V$  and  $T_c^j$  denote the true change point in this time series segment.  $\widehat{T}_c^j$  denotes the estimator of  $T_c^j$  obtained by:*

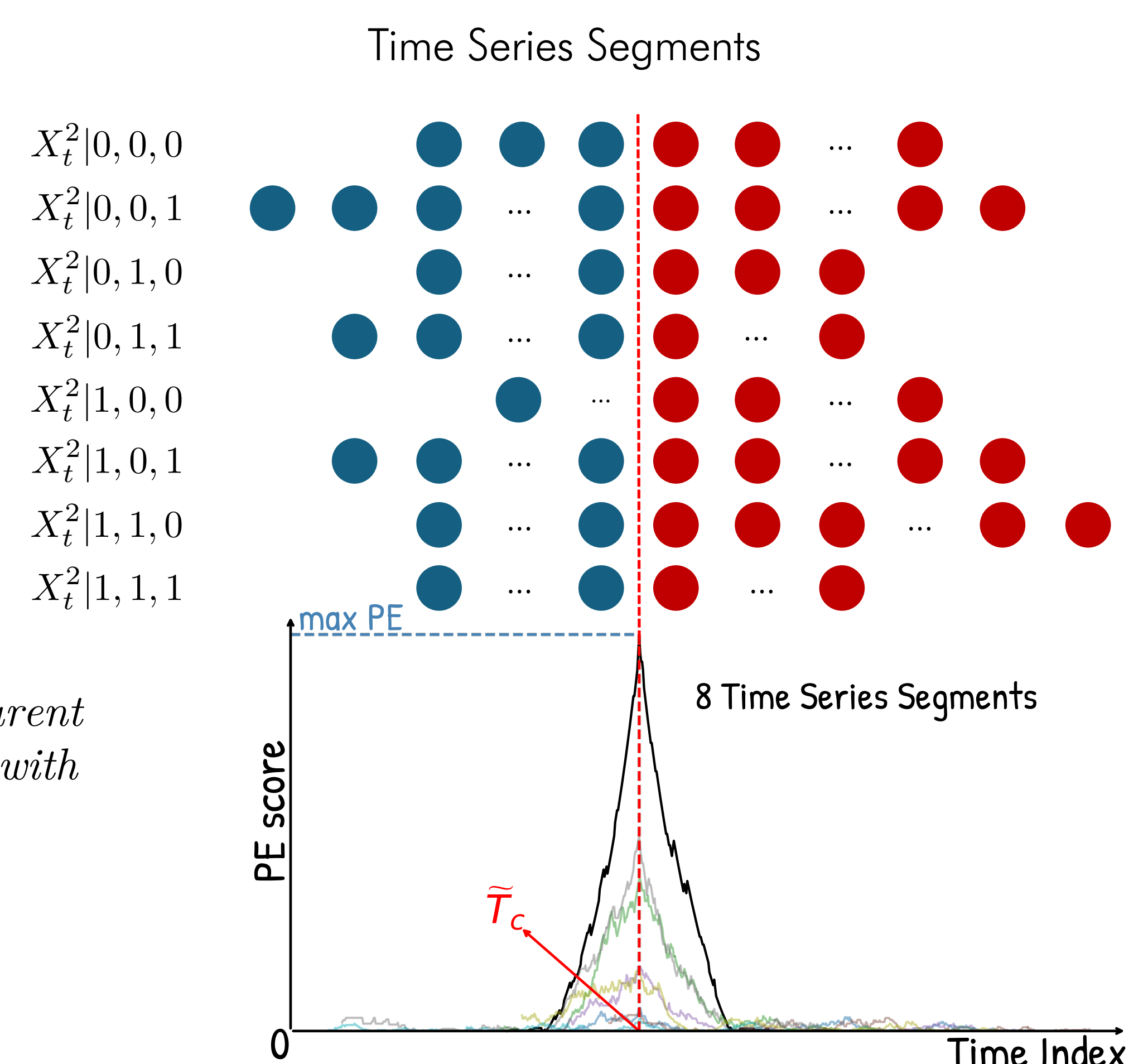
$$\widehat{T}_c^j = \arg_i \max \{\widehat{PE}_{\alpha_i}\}_i$$

*Under certain assumptions, we have that given large enough  $n_w$ ,*

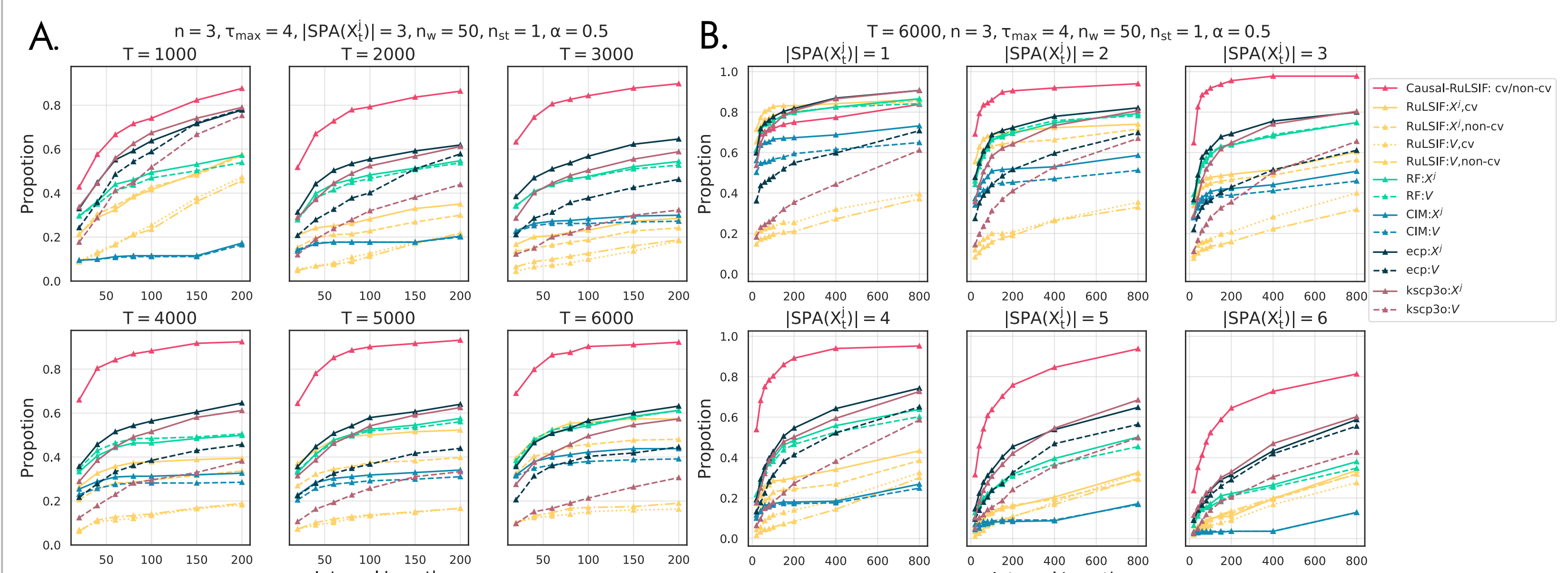
$$\Pr \left( \left| \widehat{T}_c^j - T_c^j \right| < 2n_w \right) > \left( 1 - \frac{a_w - 2}{b_{st} \log T_{sub}} - \frac{a_w}{T_{sub}} \right) \left( 1 - \frac{1}{n_w} \right)$$

where  $b_{st} = \left\lfloor \frac{\log T_{sub}}{n_{st}} \right\rfloor$ ,  $a_w = \left\lceil \frac{T_{sub}}{n_w} \right\rceil$  and  $T_{sub} := |X^j(\Lambda)|$ .

**Note:**  $n_{st}$  is the stride length, i.e., the number of time points the sliding window jumps forward at each step.  $2n_w$  is the length of the sliding window.  $\Lambda$  denotes the index of the time series segment of  $\mathbf{X}^j$ .



## Experiments



1. Proportion (Y-axis): Counts as 1 if the estimated change point falls within a specified interval (X-axis) around the true change point. The proportion is calculated over all true change points.
2. In the legend, CV: cross-validation is used to select RuLSIF hyperparameters; non-CV: no cross-validation.  $X^j$ : a univariate time series component in  $V$ ;  $V$ : the whole multivariate time series.
3. Baseline Algorithms: RuLSIF: Liu et al. (2013), CIM (Change in Mean): Vostrikova(1981), RF(ChangeForest): Lonschien et al. (2023), ecpc: James and Matteson (2013), kscpc3o: Zhang et al. (2017). Each marker represents the average accuracy over 100 random trials.

In Figure A, Causal-RuLSIF is tested with different time series lengths  $T$ , and its performance improves as the time series length  $T$  increases, empirically supporting its consistency.

In Figure B, Causal-RuLSIF is tested with different sizes of  $\text{SPA}(X_t^j)$ . It is less accurate when  $|\text{SPA}(X_t^j)| = 1$  as variables depend only on their own past  $X_{t-1}^j$ , with no cross-series correlation. When  $|\text{SPA}(X_t^j)| > 1$ , Causal-RuLSIF outperforms others by capturing shifts in causal mechanisms. However, its performance drops as  $|\text{SPA}(X_t^j)|$  increases due to the exponential growth in the total number of parent configurations, which reduces the effective sample size.

## Case Study: A Real-world Air Pollution Dataset

This dataset monitors the amount of PM<sub>10</sub> (coarse particles with a diameter between 2.5 and 10 micrometers) in the air. The 3-variate time series data records the hourly concentration of PM<sub>10</sub> across three counties in California—Fresno, Mono and Monterey—from Jan to June 2023.

During the first half of 2023, the causal mechanism of PM<sub>10</sub> in Fresno is likely to shift on May 8, 2023. While the PM<sub>10</sub> levels in Fresno and Monterey are not influenced by other counties, a causal link from Monterey to Mono has emerged after February 2, 2023.

Table 1: Causal-RuLSIF in PM<sub>10</sub> dataset

| $X$                        | $\widehat{T}_c^j$ | $\widehat{\text{PA}}(X_{t-1}^j < \widehat{T}_c^j); \widehat{\text{PA}}(X_{t-1}^j \geq \widehat{T}_c^j)$ |
|----------------------------|-------------------|---|
| $\mathbf{X}^{\text{Fr}}$   | 05/08/23          | $\{X_{t-1}^{\text{Fr}}\}; \{X_{t-1, t-2, t-3}^{\text{Fr}}\}$  |
| $\mathbf{X}^{\text{Mono}}$ | 02/01/23          | $\{X_{t-1}^{\text{Mono}}\}; \{X_{t-1, t-2, t-3}^{\text{Mono}}\}$  |
| $\mathbf{X}^{\text{Mont}}$ | 04/04/23          | $\{X_{t-1}^{\text{Mont}}\}; \{X_{t-1}^{\text{Mont}}\}$  |

## References

- [1] Gao, S., Addanki, R., Yu, T., Rossi, R. and Kocaoglu, M., 2023. Causal discovery in semi-stationary time series. *Advances in Neural Information Processing Systems*, 36, pp.46624-46657.
- [2] Runge, J., Nowack, P., Kretschmer, M., Flaxman, S. and Sejdinovic, D., 2019. Detecting and quantifying causal associations in large nonlinear time series datasets. *Science advances*, 5(11), p.eau4996.
- [3] Yamada, M., Suzuki, T., Kanamori, T., Hachiya, H. and Sugiyama, M., 2013. Relative density-ratio estimation for robust distribution comparison. *Neural computation*, 25(5), pp.1324-1370.
- [4] Liu, S., Yamada, M., Collier, N. and Sugiyama, M., 2013. Change-point detection in time-series data by relative density-ratio estimation. *Neural Networks*, 43, pp.72-83.

